Supporting Information

Polymorphism-Dependent Mechanochromic Luminescence in a Donor-Acceptor Compound

Zhi-bo Fan, Jia-wang Hou, Fei Tong*

Key Laboratory for Advanced Materials and Joint International Research Laboratory of Precision Chemistry and Molecular Engineering, Feringa Nobel Prize Scientist Joint Research Center, Frontiers Science Center for Materiobiology and Dynamic Chemistry, Institute of Fine Chemicals, School of Chemistry and Molecular Engineering, East China University of Science and Technology, 130 Meilong Road, Shanghai, 200237 (P. R. China).

E-mail addresses of corresponding authors: feitong@ecust.edu.cn

Experimental

The nuclear magnetic resonance (1H NMR and 13C NMR) spectra were recorded on the Bruker AVANCE III 500 spectrometer at 400 MHz at 298 K and tetramethyl silane (TMS) as the internal standard. HR-MS spectra were measured by using the GCT Premier TOF mass spectrometer. The UV/Vis absorption spectra data were documented by a Shimadzu UV-2600 UV-Vis spectrophotometer and the fluorescence spectra were acquired by a Shimadzu RF6000 spectrofluorophotometer. The phosphorescence spectra, fluorescence decay curves and phosphorescence decay curves were performed on a FLS1000 photoluminescence spectrometer. All PXRD data were collected on an X-ray powder diffractometer (Rigaku, 18 kW/D/Max2550VB/ PC, Cu Kα radiation, λ = 1.5418 Å, 40 kV/100 mA power) at room temperature. Single crystal X-ray diffraction (SCXRD) data were collected on a Bruker D8 VENTURE Metalet diffractometer equipped with a PHOTON III M28 detector using Gu Kα radiation (λ = 1.34139 Å).

All quantum chemical calculations were performed by using the Gaussian16 package. The molecular orbitals of MC-TPA, Type Y, Type O were obtained by density functional theory (DFT) at the level of B3LYP/6-31G (d, p). The excitation energies and natural transition orbitals (NTOs) of were performed by the time-dependent TFD (TD-DFT) calculations at the level of CAM-B3LYP /6-31G (d, p) base on crystal model and optimized isolated-state geometry

Synthesis of MC-TPA (methyl (Z)-2-cyano-3-(4-(diphenylamino)phenyl)acrylate)

A mixture of 4-formyltriphenylamine (5.00 g, 17.4 mmol) and methyl cyanoacetate (3.62 g, 36.5 mmol) was added to a stirring solution of 4-methylpiperidine (0.1 mL) in methanol (50 mL). The reaction mixture was stirred at 70 °C for 8 h. Upon completion, the mixture was cooled to room temperature, and the crude product was collected and purified by recrystallization using ice-cold methanol (50 mL) three times, affording MC-TPA as an orange powder (3.67 g, yield 73.4%). ^{1}H NMR (400 MHz, $CDCl_3$) δ: 8.10 (s, 1H), 7.89-7.80 (m, 2H), 7.40-7.31 (m, 4H), 7.24-7.14 (m, 6H), 7.01-6.93 (m, 2H), 3.90 (s, 3H). ^{13}C NMR (101 MHz, $CDCl_3$) δ: 164.18, 154.25, 152.59, 145.67, 133.25, 129.82, 126.49, 125.56, 123.31, 119.10, 116.80, 96.76, 77.35, 77.04, 76.72, 53.05. HR-MS (EI): m/z calc. for $C_{23}H_{18}N_2O_2$ $[M+H]^+$: 355.1446; found: 355.1368 (Scheme S1,Fig. S1-S3).

Preparation of single crystals for X-ray diffraction

Single crystals of the compounds reported in this study were obtained either by slow solvent evaporation or by solvent diffusion methods. Crystals of Type Y were grown by dissolving MC-TPA (10 mg) in hexane (5 mL) and allowing the solution to evaporate slowly at room temperature for 3-7 day evaporate slowly in a refrigerator. Crystals of Type O were grown by dissolving MC-TPA (10 mg) in dichloromethane /methanol (5 mL; 1 : 1 v/v) and allowing the solution to evaporate slowly at room temperature for 7 day.

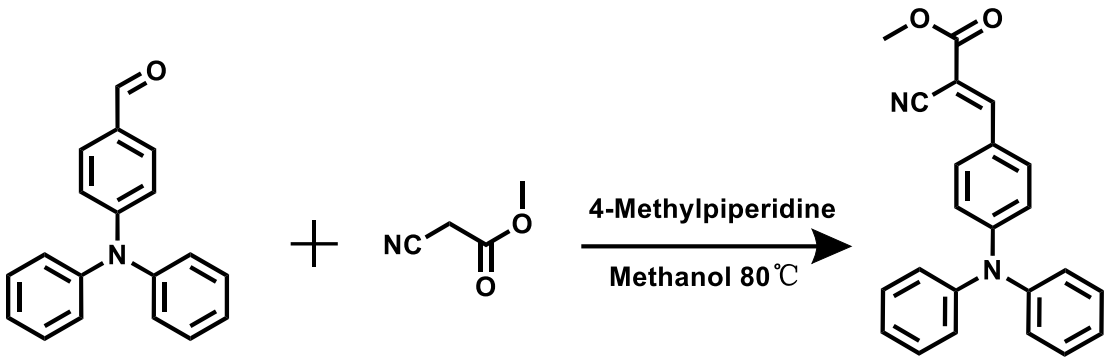

Scheme 1. Molecular structure and the corresponding synthetic procedure of MC-TPA molecule

Supporting Movie

Movie S1: MC-TPA polycrystals exhibit color and fluoresecence color changes upon grinding.

SI Figures and tables

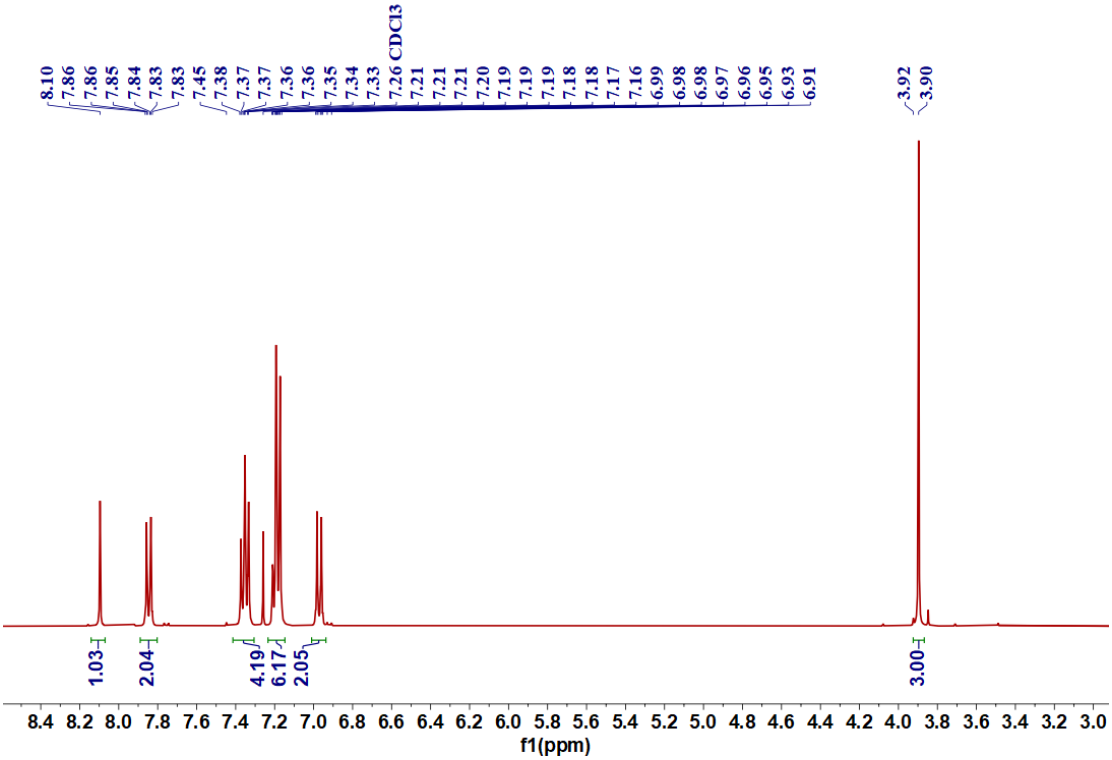

Figure S1. ^{1}H NMR spectrum of MC-TPA.

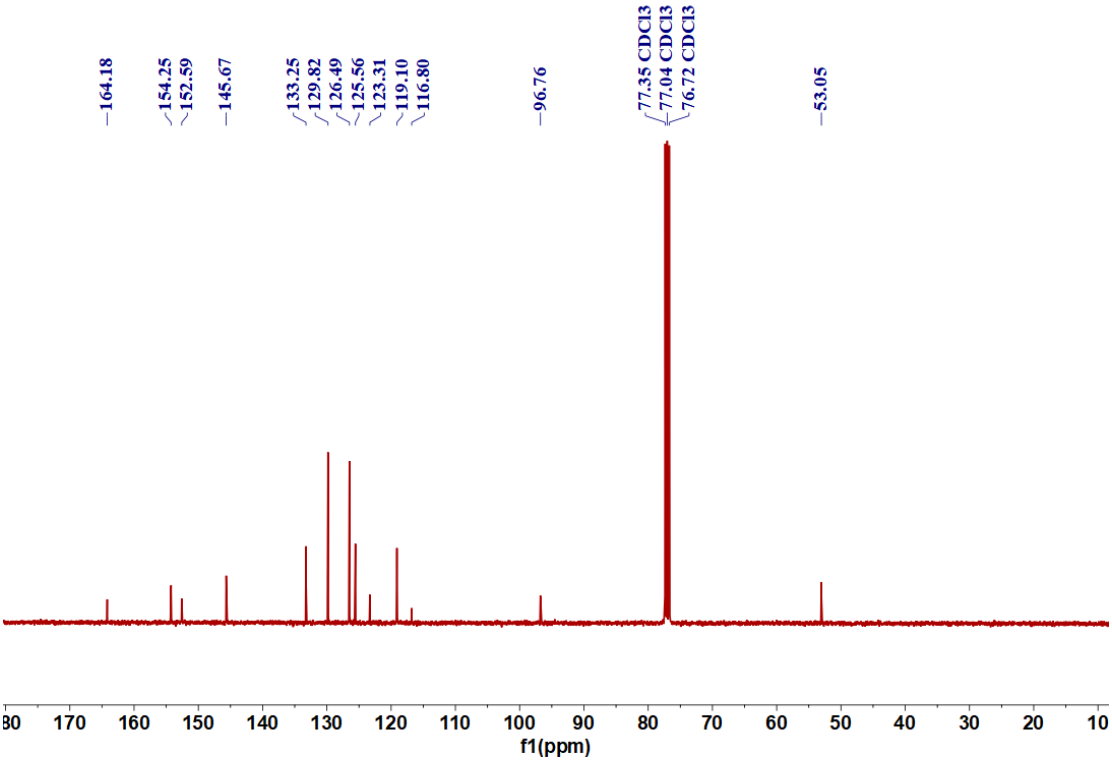

Figure S2. ^{13}C NMR spectrum of MC-TPA.

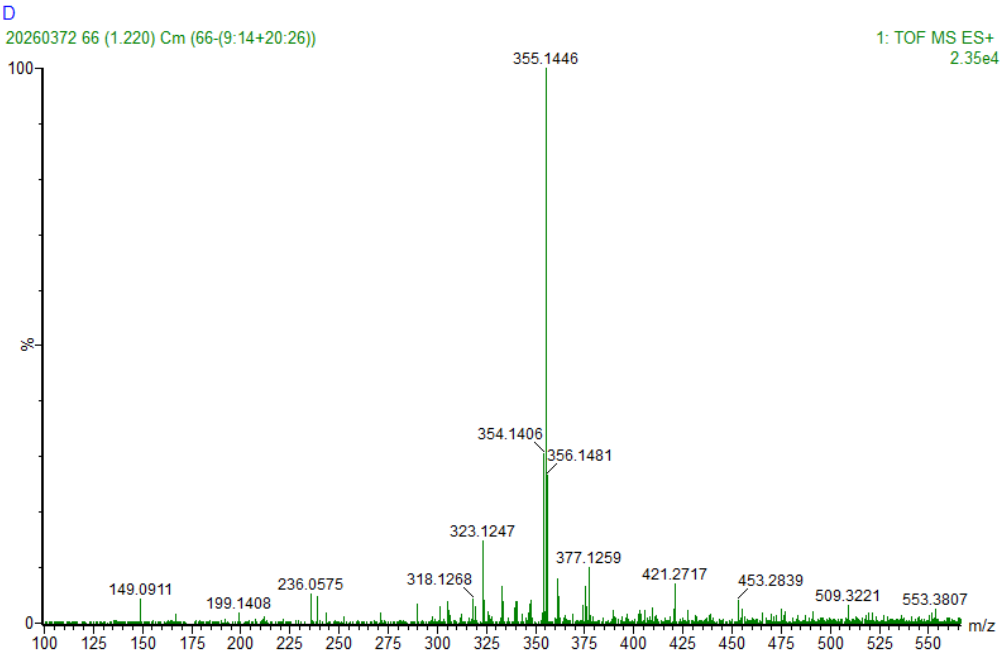

Figure S3. High-resolution mass spectrum (ESI-MS) of MC-TPA.

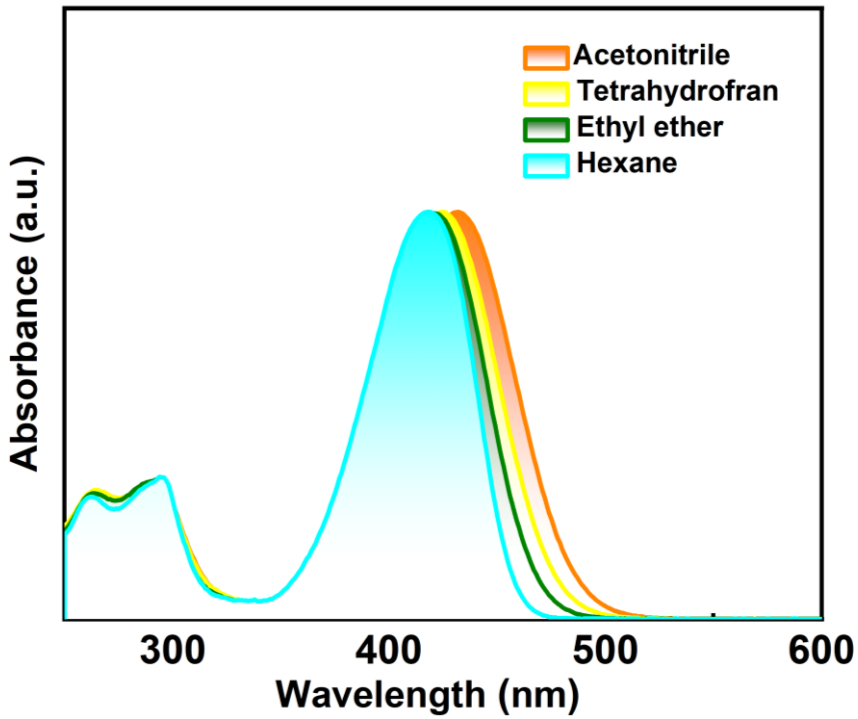

Figure S4. Absorption spectra of MC-TPA in different dilute solvents.

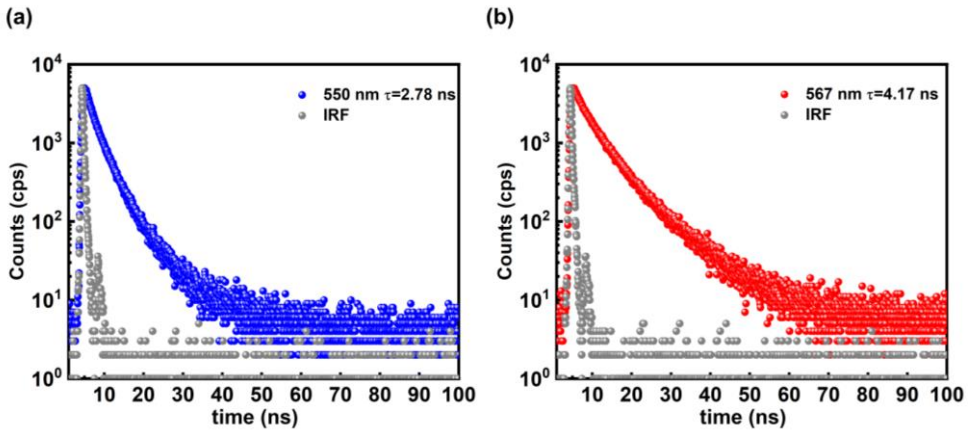

Figure S5. The detailed lifetimes data of (a) **Type Y** and (b) **Type O** crystals, and instrument response function (IRF) is included in the measurement of the fluorescence lifetime.

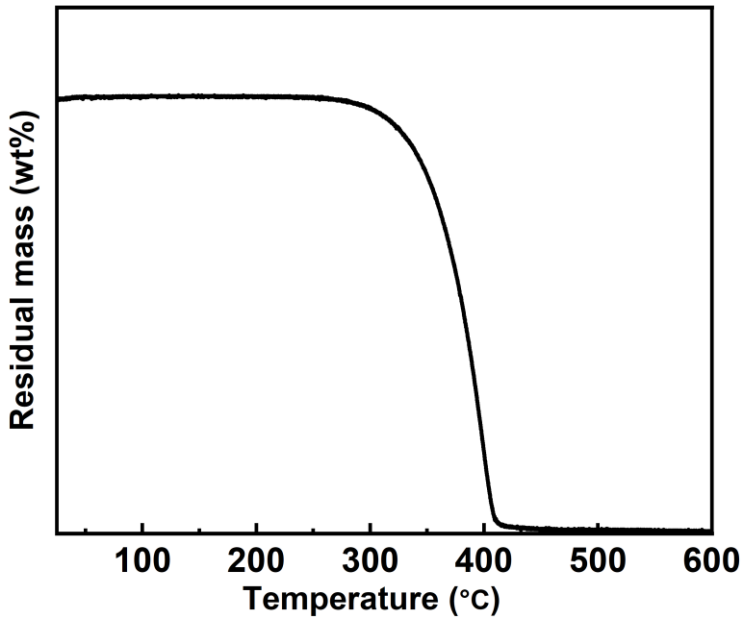

Figure S6. Thermogravimetric analysis (TGA) of MC-TPA.

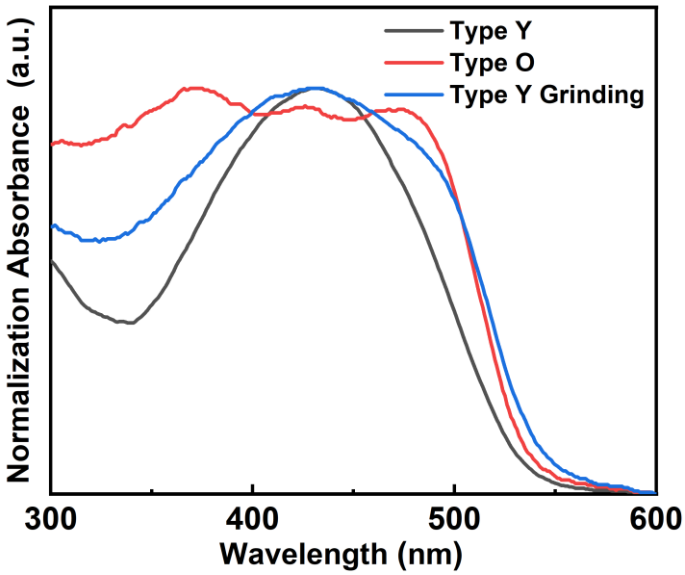

Figure S7. The UV-vis absorption spectra of **Type Y**, **Type O**, and grinding **Type Y** crystals.

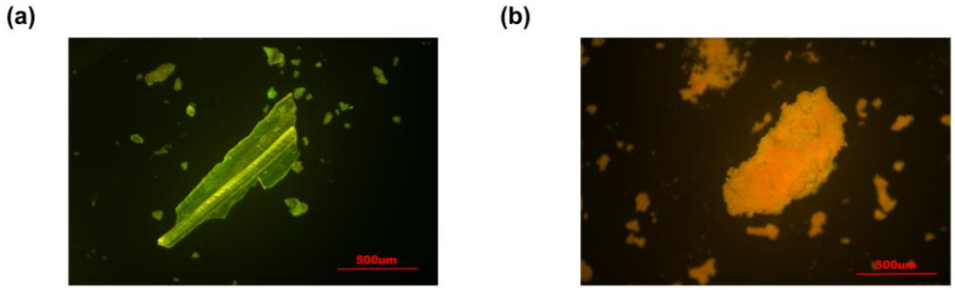

Figure S8. (a) The original single **Type Y** crystal and (b) the mechanically ground.

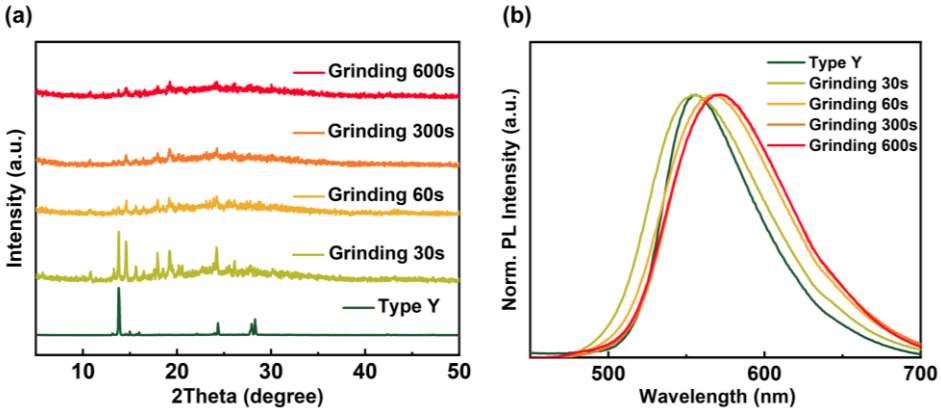

Figure S9. (a) PXRD patterns and (b) PL spectra of **Type Y** under different grinding times.

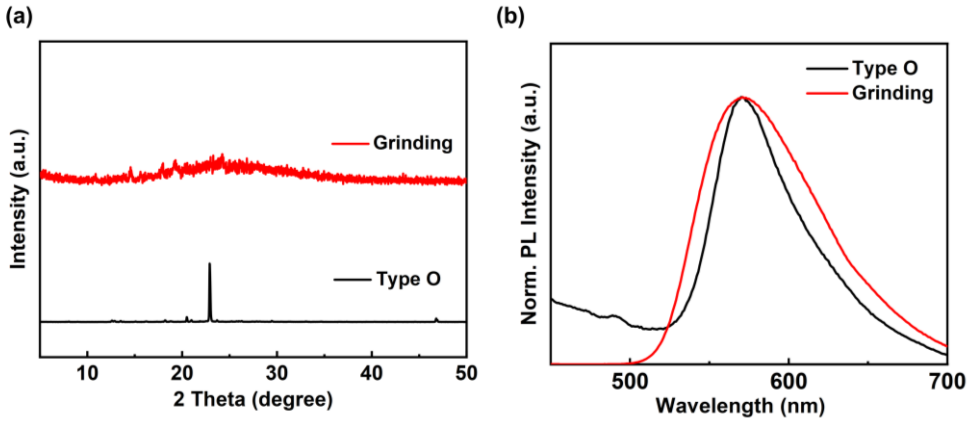

Figure S10. (a) PXRD patterns and (b) PL spectra of **Type O** under grinding

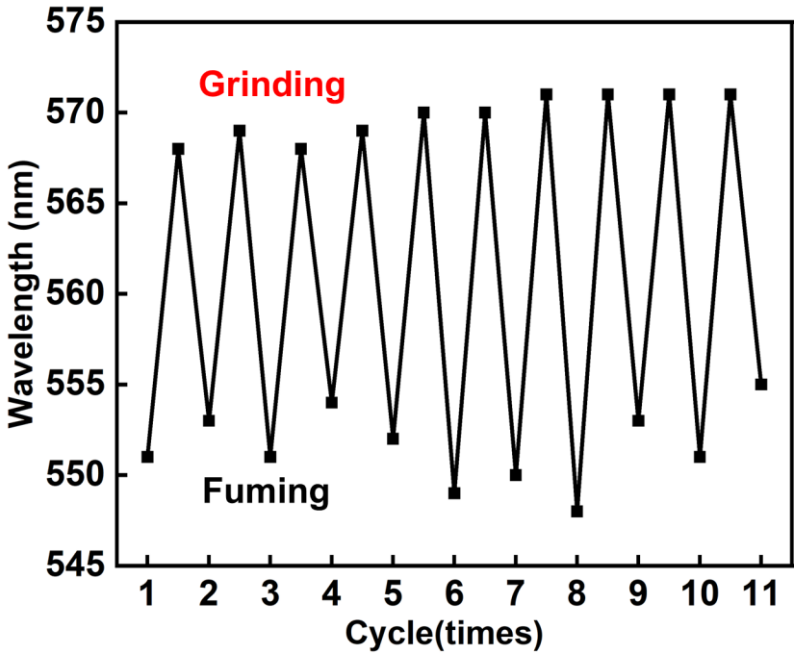

Figure S11. The maximum emission peak upon grinding and hexane fuming treatment of **Type Y**

Table S1. Crystallographic data of **Type Y** and **Type O** crystals

	Type Y	**Type O**
empirical formula	$C_{23}H_{18}N_2O_2$	$C_{23}H_{18}N_2O_2$
T [K]	150	150
crystal system	Triclinic	monoclinic
space group	P-1	P21/c
a [Å]	10.4924(4)	16.3037(17)

b [Å]	13.0953(5)	15.1986(14)
c [Å]	14.8416(5)	15.9823(14)
α [°]	67.211(2)	90
β [°]	86.293(2)	104.801(5)
γ [°]	76.380(2)	90
V [Å^3]	1826.39(12)	3828.9(6)
Z	4	8
F(000)	744	1488
density [g/cm^3]	1.289	1.230
μ [mm^{-1}]	0.66	0.63
reflections collected	37584	41330
unique reflections	7450	7461
R (int)	0.043	0.0402
GOF	1.039	1.056
R_1 [$I>2\sigma(I)$]	0.036	0.0416
ωR_2 [$I>2\sigma(I)$]	0.096	0.1172
R_1 (all data)	0.0419	0.0498
ωR2 (all data)	0.0963	0.1238

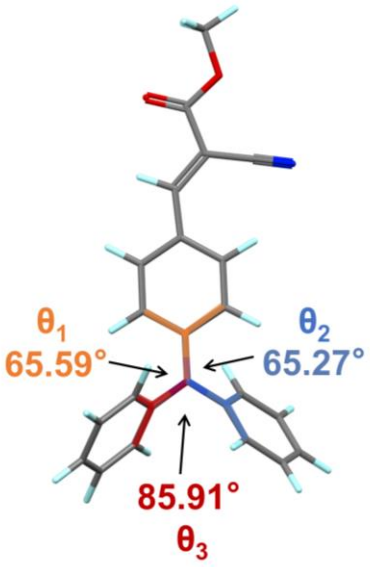

Figure S12. The dihedral angles of the triphenylamine unit in the DFT-optimized MC-TPA structure.

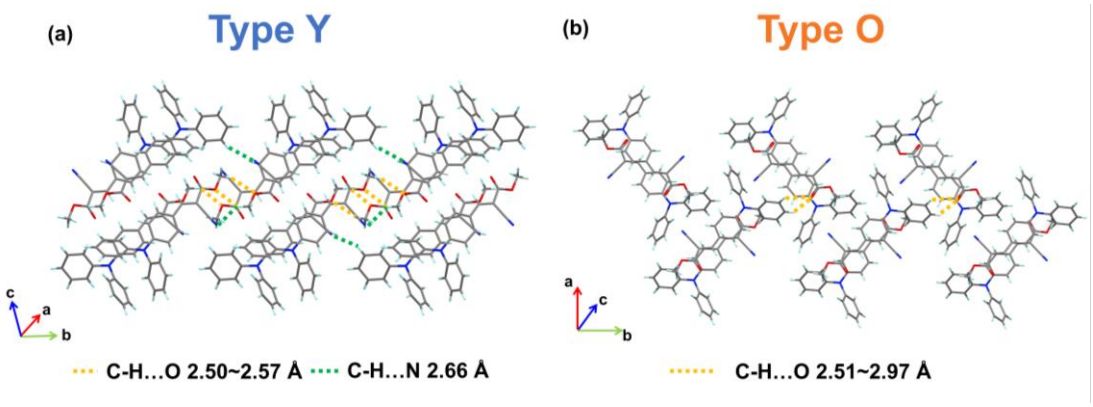

Figure S13. The intermolecular interactions between adjacent dimers in (a) **Type Y** and (b) **Type O**

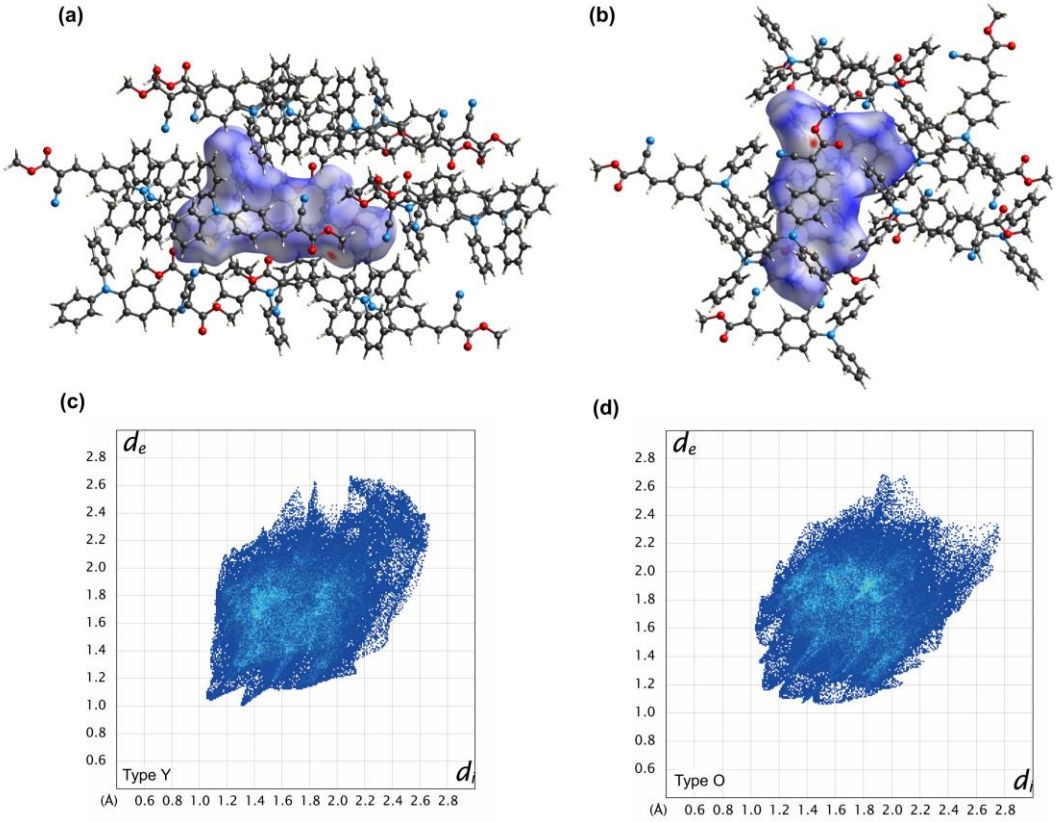

Figure S14. Hirshfeld surface of MC-TPA in (a) **Type Y** and (b) **Type O** and fingerprint plot of MC-TPA in (c) **Type Y** and (d) **Type O**.

Table S2. The proportion of different type intermolecular interactions of MC-TPA in

Type Y and **Type O**.

Intermolecular interactions	**Type Y**	**Type O**
H···H	46.5 %	49.3 %
C···H	25.4 %	27.8 %
O···H	**11.7 %**	7.7 %
N···H	**10.0 %**	8.2%
C···C	2.5 %	4%

Table S3. The energy level diagrams of **Type Y** and **Type O** crystals

	LUMO (eV)	HOMO (eV)	Gap Energy (eV)
Type Y	-1.89	-5.15	3.25
Type O	-2.09	-4.99	2.90

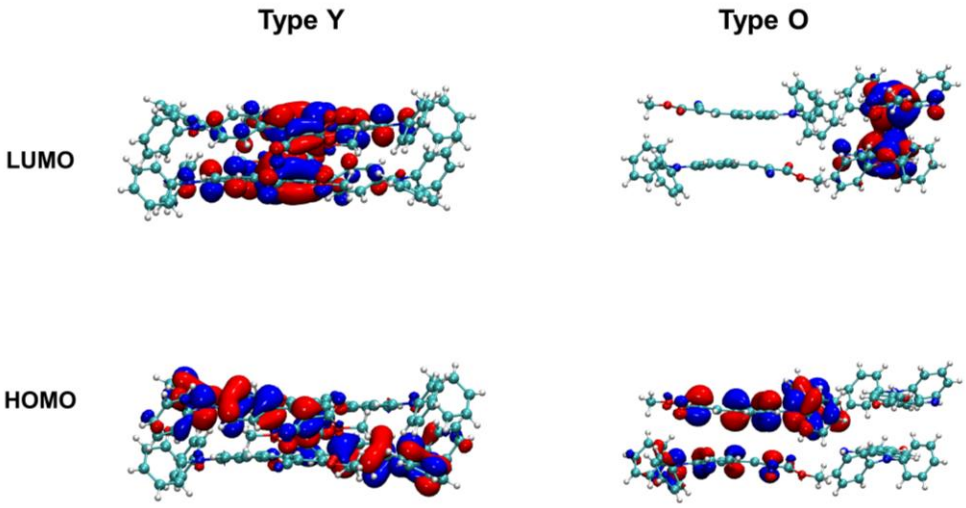

Figure S15. Frontier molecular orbitals of **Type Y** and **Type O** crystals.

Table S4. Contributions of each monomer to the hole and particle in **Type Y** crystals

	Monomer 1	Monomer 2	Monomer 3	Monomer 4
Hole	0.78 %	0.76 %	**48.86 %**	**49.60 %**
Particle	**47.00 %**	**46.92 %**	3.05 %	3.04 %

Table S5. Contributions of each monomer to the hole and particle in **Type O** crystals

	Monomer 1	Monomer 2	Monomer 3	Monomer 4
Hole	0.06 %	7.15 %	**92.68 %**	0.11 %
Particle	**45.67 %**	0.01 %	0.16 %	**54.16 %**

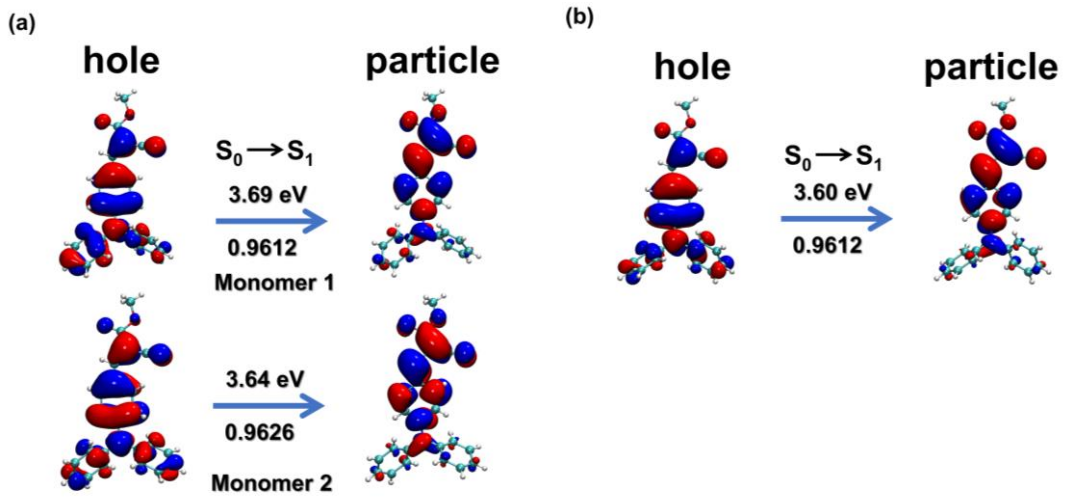

Figure S16. The NTOs of Monomer in (a) **Type Y** and (b) DFT-optimized MC-TPA structure.